BMJ Open

Geometric uncertainty in intracranial aneurysm rupture status discrimination: a two-site retrospective study

Florian Hellmeier,[1] Jan Brüning ,[1] Philipp Berg,[2,3] Sylvia Saalfeld,[3,4] Andreas Spuler,[5] Ibrahim Erol Sandalcioglu,[6] Oliver Beuing,[7] Naomi Larsen,[8] Jens Schaller,[1] Leonid Goubergrits [1,9]

To cite: Hellmeier F, Brüning J, Berg P, *et al*. Geometric uncertainty in intracranial aneurysm rupture status discrimination: a two-site retrospective study. *BMJ Open* 2022;**12**:e063051. doi:10.1136/bmjopen-2022-063051

► Prepublication history and additional supplemental material for this paper are available online. To view these files, please visit the journal online (http://dx.doi.org/10.1136/bmjopen-2022-063051).

Received 23 March 2022
Accepted 09 October 2022

For numbered affiliations see end of article.

Correspondence to
Dr Jan Brüning;
jan.bruening@charite.de

ABSTRACT

Objectives Assessing the risk associated with unruptured intracranial aneurysms (IAs) is essential in clinical decision making. Several geometric risk parameters have been proposed for this purpose. However, performance of these parameters has been inconsistent. This study evaluates the performance and robustness of geometric risk parameters on two datasets and compare it to the uncertainty inherent in assessing these parameters and quantifies interparameter correlations.

Methods Two datasets containing 244 ruptured and unruptured IA geometries from 178 patients were retrospectively analysed. IAs were stratified by anatomical region, based on the PHASES score locations. 37 geometric risk parameters representing four groups (size, neck, non-dimensional, and curvature parameters) were assessed. Analysis included standardised absolute group differences (SADs) between ruptured and unruptured IAs, ratios of SAD to median relative uncertainty (MRU) associated with the parameters, and interparameter correlation.

Results The ratio of SAD to MRU was lower for higher dimensional size parameters (ie, areas and volumes) than for one-dimensional size parameters. Non-dimensional size parameters performed comparatively well with regard to SAD and MRU. SAD was higher in the posterior anatomical region. Correlation of parameters was strongest within parameter (sub)groups and between size and curvature parameters, while anatomical region did not strongly affect correlation patterns.

Conclusion Non-dimensional parameters and few parameters from other groups were comparatively robust, suggesting that they might generalise better to other datasets. The data on discriminative performance and interparameter correlations presented in this study may aid in developing and choosing robust geometric parameters for use in rupture risk models.

STRENGTHS AND LIMITATIONS OF THIS STUDY

⇒ This study provides location-specific estimates of the discriminative ability of a large set of geometric parameters for intracranial aneurysm rupture status assessment, while also considering uncertainty.
⇒ The analysis was performed on two independent datasets to assess robustness of the findings.
⇒ Even though the relative uncertainty in acquisition of each geometric risk parameter was evaluated based on more than 20 individual segmentations performed during the Multiple Aneurysms Anatomy Challenge, this evaluation was only performed on five aneurysms in total.

INTRODUCTION

A relevant part of the general population harbours one or more unruptured intracranial aneurysms (IAs), with the overall prevalence estimated around 3%.[1] While most IAs do not rupture,[2] the question of whether and when to treat them remains relevant due to the poor prognosis of ruptured IAs[3 4] as well as the risk of intervention.[3 5] Current American Heart Association/American Stroke Association guidelines list several modifiable and non-modifiable risk factors for IA growth and/or rupture, including IA location, growth rate, morphology, smoking status, alcohol consumption, hypertension, age, sex, previous IA, and family history.[6] Attempts have been made to develop scoring systems to quantify rupture risk, growth risk, and/or support treatment decisions; these include the PHASES score by Greving *et al*,[7] the UIATS by Etminan *et al*[8], and the ELAPSS score by Backes *et al*.[9] All three of these scores are based on clinically available data and all include geometric rupture risk parameters: IA size in case of the PHASES score,[7] surface irregularity, size ratio, as well as aspect ratio in case of the UIATS[8], and IA size as well as surface irregularity for the ELAPSS score.[9] While these metrics were designed to support clinical decision making, performance on clinical data has been mixed,[10–12] and improvements, particularly for patients harbouring multiple IAs, are desired by clinicians.[13]

The aim of this paper is to assess the ability of a broad number of proposed geometric risk parameters to differentiate between

unruptured and ruptured IAs while also comparing their discriminative ability relative to the uncertainty encountered in determining them. Any acquisition of patient-specific IA geometries and subsequent use of these geometries to derive geometric risk parameters is affected by a number of uncertainty-introducing factors. These include the medical imaging acquisition itself, which is followed by image data preprocessing, segmentation, geometry reconstruction including postprocessing (eg, smoothing, checking of topology), and finally calculation of the geometric risk parameters. All these processing steps are associated with some errors, resulting in uncertainty, which negatively affects the ability of parameters to discriminate IA rupture status. Discrimination of rupture status on an individual IA level is, however, necessary if these parameters are to support the clinical decision-making process, including any decisions regarding treatment modalities. Previous studies found high variability in the uncertainty of different geometric risk parameters as well as differences in their ability to differentiate between ruptured and unruptured IAs.[14–16] Furthermore, for geometric risk parameters with multiple alternative definitions, the specific implementation can affect the discriminative performance of the parameter itself and any derived parameters, as demonstrated by Lauric *et al* for parameters incorporating IA and neck size.[17]

The current study was performed to facilitate optimal selection of geometric rupture risk parameters by identifying geometric parameters, which are good discriminators while also exhibiting low uncertainty. The analysis is performed on two datasets processed by different research groups and is differentiated by anatomical region, in order to assess how the rupture status discrimination of the geometric parameters is affected by geometry processing as well as anatomical location. Additionally, correlation of the geometric risk parameters with each other is assessed.

METHODS

Medical imaging data

IA geometries were retrospectively reconstructed and segmented from three-dimensional (3D) rotational angiography data acquired for routine clinical indications. Data were collected consecutively. The inclusion criteria of the datasets were imaging modality and the corresponding acquisition resolution. Cases with considerable segmentation artefacts such as close vessels that appear to be merged or holes in the segmented lumen were rejected from the analysis. 142 IAs were acquired in the Helios Klinikum Berlin-Buch (Berlin, Germany), 38 in KRH Klinikum Nordstadt (Hanover, Germany), 23 in the University Medical Center Schleswig-Holstein (UKSH) (Kiel, Germany) and 41 in the University Hospital Magdeburg (Magdeburg, Germany). Processing of the imaging data, including segmentation, was performed at two sites: Berlin, which processed 142 IAs from Helios Klinikum Berlin-Buch (dataset 1), and Magdeburg, which processed 102 IAs from KRH Klinikum Nordstadt, UKSH and University Hospital Magdeburg (dataset 2). Overall, 244 IAs from 178 patients were included, from which geometric risk parameters were subsequently calculated. Based on the PHASES score,[7] aneurysm location was classified into four anatomical regions: internal carotid artery (ICA), middle cerebral artery (MCA), anterior region (all vessels anterior of the ICA/MCA) and posterior region (all vessels posterior of the ICA/MCA). The distribution of the individual IA locations and their assignment to the four anatomical regions are shown in table 1.

Table 1 Frequency and rupture status of individual IA locations by dataset

Anatomical region	Vessel	Dataset 1 unruptured	Dataset 1 ruptured	Dataset 2 unruptured	Dataset 2 ruptured
Anterior	ACA	3	1	2	2
	AComA	10	22	11	5
ICA	AChA	0	1	1	2
	ICA	29	8	19	4
MCA	MCA	28	10	31	8
Posterior	PComA	8	10	2	4
	PCA	0	1	0	0
	SCA	0	0	1	1
	BA	4	3	3	4
	PICA	0	4	1	0
	VA	0	0	0	1

ACA, anterior cerebral artery; AchA, anterior choroidal artery; AComA, anterior communicating artery; BA, basilar artery; IA, intracranial aneurysm; ICA, internal carotid artery; MCA, middle cerebral artery; PCA, posterior cerebral artery; PComA, posterior communicating artery; PICA, posterior inferior cerebellar artery; SCA, superior cerebellar artery; VA, vertebral artery.

Geometric risk parameters

Historically, several geometric parameters for IA rupture risk assessment have been proposed. In order to have access to information on parameter uncertainty, the parameters chosen for this study were limited to a subset of the parameters reported in Goubergrits *et al*,[14] a parameter uncertainty study performed on segmentation data obtained during the Multiple Aneurysms AnaTomy Challenge (MATCH) 2018.[18] The major outcome of this study was the median relative uncertainty (MRU) of geometric parameters. Briefly, five aneurysms were segmented and reconstructed by 26 international research groups, which participated in the MATCH challenge. These segmentations were used to calculate the median and the 68.3% range between the 84.13th and the 15.87th percentile of all selected geometric parameters for each of the five aneurysms. The uncertainty range was selected with respect to the range of ±1 SD for normally distributed data reported in other studies. The uncertainty was defined as the uncertainty range divided by the median value and calculated for each geometric parameter. Finally, the average of all five aneurysms was calculated to define the MRU. For a detailed description of the parameters and the rationale for choosing the parameters, the interested reader is referred to Goubergrits *et al*.[14] Briefly, most of the proposed geometric parameters describe aneurysm and/or aneurysmal neck size or shape or irregularity. These parameters were previously proposed as predictors for rupture risk. Table 2 lists the geometric parameters, their abbreviations and MRU values, as well as their respective references.

Since the diameter of the parent vessel was not available for all IAs studied, size ratio could not be calculated and was excluded. Furthermore, UI and convexity ratio (CR) as well as NSI and isoperimetric ratio (IPR) are directly related through $CR = 1 - UI$ and $IPR = \frac{\sqrt[3]{18\pi}}{1-NSI}$, respectively. CR and IPR were therefore not included in the analysis, in order to avoid redundancy. Geometric risk parameters were calculated from the IA geometries using MATLAB (version R2017b, MathWorks, Natick, USA), Python (version 3.7.1, Python Software Foundation, Delaware, USA) and ZIBAmira (version 2015.28, Zuse Institute Berlin, Berlin, Germany). The individual parameter values, IA location, and rupture status for each IA in this study, as well as the exact values of the interparameter correlation coefficients are provided as online supplemental file 1, online supplemental file 2 respectively.

Statistical analysis

Since most of the geometric risk parameters were non-normally distributed, as assessed by Q–Q plots and Shapiro-Wilk tests, the median was used to quantify central tendency and interquartile range (IQR) was used to quantify dispersion. Correlations were quantified using Pearson's r with correlations $|r| \geq 0.75$ referred to as strong, while those with $0.75 > |r| \geq 0.25$ and $|r| < 0.25$ referred to as moderate and weak, respectively. Statistical analysis was performed using SPSS (version 28.0.0.0, IBM, Armonk, USA) and MATLAB.

The discriminative ability of the individual parameters was assessed by standardising the absolute difference between the medians of the ruptured and unruptured IAs with the weighted arithmetic mean of the IQRs of the two groups. This measure of effect size will be referred to as the standardised absolute group difference (SAD). Furthermore, the ratio of the SAD to the median relative uncertainty (MRU), a measure of the uncertainty associated with parameter calculation, from Goubergrits *et al*[14] was calculated for all parameters and will be referred to as the group difference–uncertainty ratio (DUR). The equations for SAD and DUR are thus $SAD = \frac{(n_r+n_u)\cdot|m_r-m_u|}{n_rIQR_r+n_uIQR_u}$ and $DUR = \frac{SAD}{MRU}$, where n_i, m_i, and IQR_i are the sample sizes, median values, and IQRs of the geometric parameters evaluated for ruptured (subscript r) and unruptured (subscript u) samples, while MRU is the median relative uncertainty from Goubergrits *et al*,[14] which is also listed in table 2. SAD and DUR may take any value ≥0 with higher values indicating stronger discriminative ability and a better ratio of discriminative ability to uncertainty, respectively. SAD and DUR values of zero would indicate no discriminative ability and the worst possible ratio of discriminative ability to uncertainty, respectively. Additionally, the correlation coefficients between the parameters were calculated. Analysis of SAD and DUR as well as the correlation coefficients was performed individually for each anatomical region and each dataset.

Patient and public involvement

Due to the purely retrospective manner of this study, no involvement of patients or the general public was considered.

RESULTS

Figure 1 shows SAD for all geometric risk parameters by anatomical region and dataset. Considering both datasets, the following parameters achieved the comparatively highest SAD for each anatomical region: curvature (HMC, MLN, HGC, GLN) and non-dimensional (AR, eAR, AVSV, AASA) parameters in the anterior region, curvature (HMC, HGC) and non-dimensional (NSI, AASA, EI) parameters in the ICA, non-dimensional (AR, eAR, BL, AVSV, AASA) parameters in the MCA, and size (H, L_{max}, A, A_{MBS}) and curvature (MSD, absGAA, GSD) parameters in the posterior region. Compared with the other anatomical regions, SAD was higher in the posterior region, and more parameters exhibited relatively high SAD. Looking at all anatomical regions combined, curvature (HMC, MLN, absGAA, HGC, GLN) and non-dimensional (AR, eAR, AVSV, AASA) parameters as well as one neck ($D_{neck,min}$) and one size (H_b) parameter show comparatively high SAD in both datasets. Furthermore, the differences between the two datasets become less pronounced when combining all anatomical regions. Moreover, this combined evaluation resulted in SAD

Table 2 List of the investigated geometric parameters, their descriptions, and median relative uncertainties (MRUs)

Parameter group	Parameter name, unit (exemplary reference)	Parameter abbreviation	Short description	MRU
Size	Height, mm[19]	H	Maximum perpendicular distance from the neck plane to the aneurysm surface	0.140
	Maximum dimension, mm[32]	L_{max}	Maximum distance between two points on the aneurysm surface	0.157
	Maximum height, mm[15]	H_{max}	Maximum distance between the centroid of the neck and the aneurysm surface	0.123
	Maximum diameter, mm[17]	D_{max}	Maximum neck plane-parallel distance between two points on the aneurysm surface	0.169
	Bulge height, mm[19]	H_b	Distance between the neck plane and the maximum diameter	0.373
	Surface area, mm^2[15]	A	Surface area of the aneurysm	0.215
	Convex hull surface area, mm^2[15]	A_{CH}	Surface area of the aneurysm's convex hull	0.277
	Minimal bounding sphere surface area, mm^2[33]	A_{MBS}	Surface area of the aneurysm's minimal bounding sphere	0.305
	Closed surface area, mm^2	A_{closed}	Surface area of the neck-closed aneurysm	0.283
	Volume, mm^3[15]	V	Volume of the neck-closed aneurysm	0.392
	Convex hull volume, mm^3[15]	V_{CH}	Volume of the aneurysm's convex hull	0.399
	Minimal bounding sphere volume, mm^3[33]	V_{MBS}	Volume of the aneurysm's minimal bounding sphere	0.451
Neck	Minimum neck diameter, mm[17]	$D_{neck,min}$	Minimum distance between two opposite points on the neck perimeter	0.306
	Maximum neck diameter, mm[34]	$D_{neck,max}$	Maximum distance between two points on the neck perimeter	0.348
	Neck perimeter, mm[19]	P_{neck}	Perimeter of the aneurysm neck	0.374
	Equivalent neck diameter, mm[19]	$D_{neck,equiv}$	Hydraulic diameter of the aneurysm neck	0.276
	Neck area, mm^2[19]	A_{neck}	Area of the aneurysm neck	0.593
	Elliptical neck area, mm^2	$A_{neck,elliptical}$	Neck area calculated as the product of the minimum and maximum neck diameter	0.650
Non-dimensional	Aspect ratio[34]	AR	Ratio of height to maximum neck diameter	0.293
	Equivalent aspect ratio[19]	eAR	Ratio of height to equivalent neck diameter	0.326
	Bottleneck factor[19]	BF	Ratio of maximum diameter to maximum neck diameter	0.201
	Bulge location[19]	BL	Ratio of bulge height to height	0.301
	Nonsphericity index[15]	NSI	Normalised ratio of volume to surface area relative to a hemisphere	0.108
	Aneurysm volume to bounding sphere volume[33]	AVSV	Ratio of volume to minimal bounding sphere volume	0.173
	Aneurysm surface area to bounding sphere area[33]	AASA	Ratio of surface area to minimal bounding sphere surface area	0.095
	Undulation index[15]	UI	1 minus the ratio of volume to convex hull volume	0.709
	Ellipticity index[15]	EI	Normalised ratio of convex hull volume to convex hull surface area relative to a hemisphere	0.051

Continued

Table 2 Continued

Parameter group	Parameter name, unit (exemplary reference)	Parameter abbreviation	Short description	MRU
Curvature	Mean of mean curvature, mm^{-1}[19]	MAA	Surface average of local mean curvature	0.136
	Mean of absolute mean curvature, mm^{-1}	absMAA	Surface average of the magnitude of the local mean curvature	0.133
	SD of mean curvature, mm^{-1}	MSD	SD of the local mean curvature	1.011
	High mean curvature, %[33]	HMC	Relative increase of the mean of absolute mean curvature over the mean curvature of the minimal bounding sphere	0.396
	L2-norm of mean curvature[19]	MLN	Scale invariant measure of surface irregularity, uses mean curvature	0.150
	Mean of Gaussian curvature, mm^{-2}[19]	GAA	Surface average of local Gaussian curvature	0.344
	Mean of absolute Gaussian curvature, mm^{-2}	absGAA	Surface average of the magnitude of the local Gaussian curvature	0.485
	SD of Gaussian curvature, mm^{-2}	GSD	SD of the local Gaussian curvature	1.798
	High Gaussian curvature, %[33]	HGC	Relative increase of the mean of absolute Gaussian curvature over the Gaussian curvature of the minimal bounding sphere	0.822
	L2-norm of Gaussian curvature[19]	GLN	Scale invariant measure of surface irregularity, uses Gaussian curvature	0.545

Note that terminology and implementation in the references might differ subtly. Derived and modified from tables 1–5 from Goubergrits *et al*,[14] used under Creative Commons Attribution License (CC BY 4.0). The CC BY 4.0 license text is available at https://creativecommons.org/licenses/by/4.0/.
MRU, median relative uncertainty.

being higher for the size parameters in site 2 compared with site 1. Here, it is worthwhile to note that the SAD of this combined assessment is not the average of the SAD of all four region-specific evaluations. Thus, pooling for some parameters can result in the absolute difference between the ruptured and unruptured groups to be close to zero, which results in SAD values close to zero as observed for the one-dimensional size parameters of the site 1 dataset.

Figure 2 shows DUR for all geometric risk parameters by anatomical region and dataset. Considering both datasets, the following parameters achieved the comparatively highest DUR for each anatomical region: non-dimensional (AASA, EI) and one curvature (MLN) parameter in the anterior region, non-dimensional (EI, AASA, NSI) parameters in the ICA, non-dimensional (AASA, EI) parameters in the MCA, and size (H, L_{max}, H_{max}, A), curvature (MAA, absMAA), and one non-dimensional (EI) parameter in the posterior region. Similar to SAD, DUR in the posterior region was overall higher and more parameters exhibited relatively high DUR, compared with the other anatomical regions. Looking at all anatomical regions combined, non-dimensional (NSI, AVSV, AASA, EI) and curvature (absMAA, MLN) parameters show comparatively high DUR in both datasets. As for SAD, the differences between the two datasets are less pronounced when looking at all anatomical regions combined.

Figures 3 and 4 show correlation coefficients between the geometric risk parameters by anatomical region for both datasets. The following general features are present in most data correlation plots: The size parameters (H, L_{max}, H_{max}, D_{max}, H_b, A, A_{CH}, A_{MBS}, A_{closed}, V, V_{CH}, V_{MBS}) are generally strongly correlated with each other. Similarly, the neck parameters ($D_{neck,min}$, $D_{neck,max}$, P_{neck}, $D_{neck,equiv}$, A_{neck}, $A_{neck,elliptical}$) are also generally strongly correlated with each other.

Within the non-dimensional parameter group, there are two distinct subgroups in most plots: one formed by AR, eAR, BF and BL and one formed by NSI, AVSV, AASA, UI and EI. Within the latter subgroup, several of the correlations are negative, but their magnitude is overall moderate to strong. The curvature parameters also form two subgroups: one formed by dimensional curvature parameters (MAA, absMAA, MDS, GAA, absGAA, GSD) and one by non-dimensional curvature parameters (HMC, MLN, HGC, GLN). With regard to correlations between parameter groups, there is generally moderate to strong correlation between the size and neck parameters. Additionally, the size and neck parameters are generally moderately correlated with the curvature parameters, the direction of the correlation being positive for the non-dimensional curvature parameters and negative for the dimensional curvature parameters.

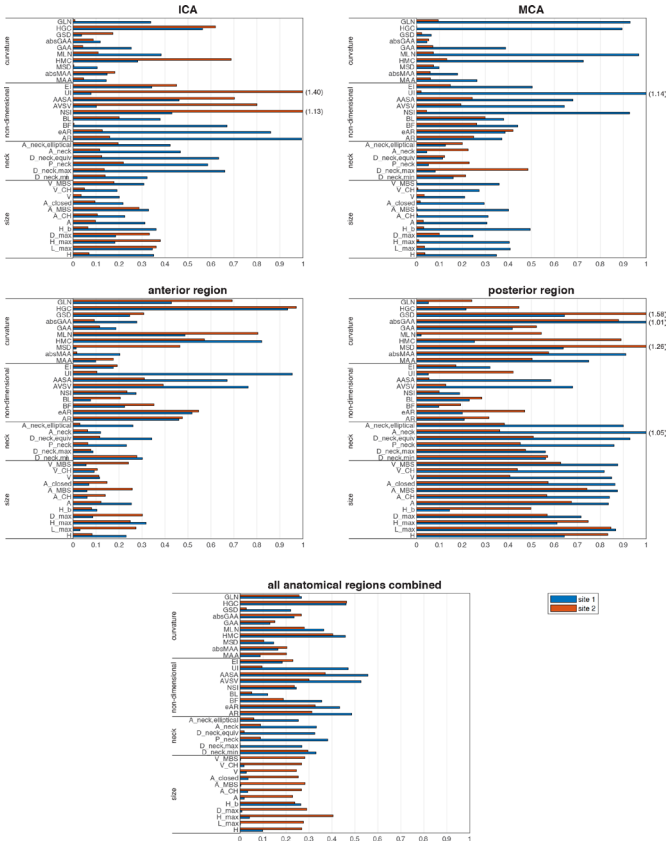

Figure 1 Standardised absolute group difference (SAD) for each anatomical region and dataset.

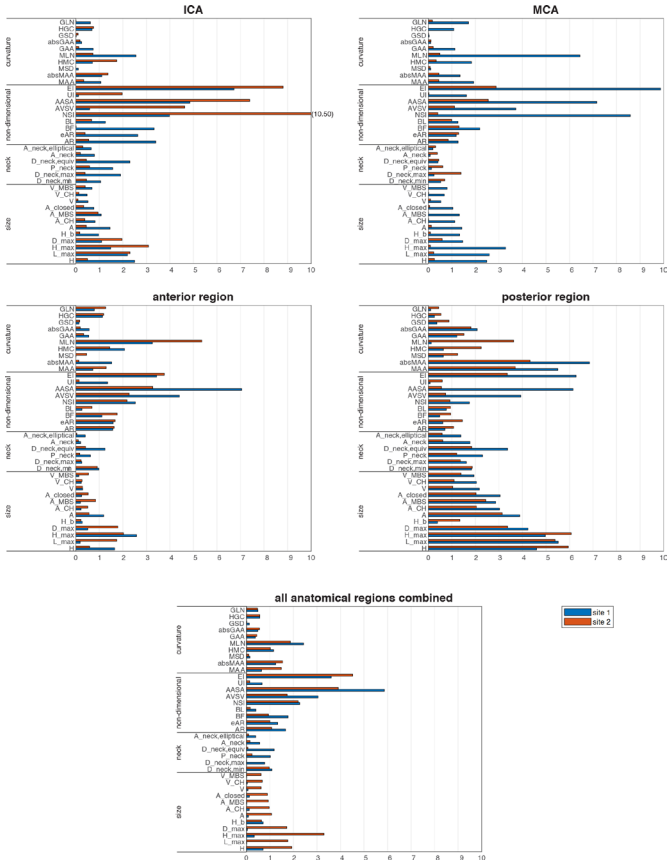

Figure 2 Group difference–uncertainty ratio (DUR) for each anatomical region and dataset. ICA, internal carotid artery; MCA, middle cerebral artery.

DISCUSSION

Previous research has assessed the impact of uncertainty on geometric risk parameters in a limited fashion. Ma *et al*[19] examined the influence of random noise on the calculation of 14 geometric risk parameters, finding curvature parameters more susceptible to random noise than size, neck, and non-dimensional parameters. Others have examined the influence of imaging modality[20] and CT angiography reconstruction kernel[21] on geometric risk parameters. Regarding image acquisition, Ramachandran *et al*[20] have examined the influence of imaging modality while O'Meara *et al*[21] and Berg *et al*[22] have focused on the reconstruction kernel's effect on geometric and haemodynamic risk parameters, respectively. The current study as well as the earlier uncertainty study based on the MATCH challenge[14] were both based on 3D rotational angiography imaging, which is the routine imaging modality in both centres involved in this study. Other sensitivity and uncertainty aspects of computational fluid dynamics approaches to IAs have been explored, for example, by Cebral *et al*,[23] Sarrami-Foroushani *et al*[24], and Schneiders *et al*.[25] To the authors' knowledge, there is, however, no comprehensive publication relating discriminative performance and uncertainty of geometric risk parameters, while also providing detailed data on their correlation with each other.

Looking at the parameter groups examined in this study, the following findings can be made: the size and neck parameters measuring areas (A, A_{CH}, A_{MBS}, A_{closed}, A_{neck}, $A_{neck,elliptical}$) and volumes (V, V_{CH}, V_{MBS}) generally do not achieve high DUR, despite having SAD similar to the size and neck parameters measuring length (H, L_{max}, H_{max}, D_{max}, H_b, $D_{neck,min}$, $D_{neck,max}$, P_{neck}, $D_{neck,equiv}$). The cause is the higher uncertainty encountered in determining the higher dimensional parameters when compared with the one-dimensional parameters.[14] This suggests that higher-dimensional size parameters tend to be less robust and thus less suitable for use in practical risk models than one-dimensional size parameters. Like Lauric *et al*,[17] there are instances of noticeable differences in the discriminative performance of parameters capturing the same aspect of IA geometry, for example, for the neck size parameters. The non-dimensional parameters exhibit comparatively high SAD and DUR, except for BL and UI, which exhibit lower discriminative ability and/or higher uncertainty in their calculation. The curvature parameters show substantial variability in SAD and DUR depending on the anatomical region and the parameter, with MLN performing comparatively well overall. It is notable that the posterior region tends to exhibit higher SAD and DUR than the other regions, indicating more pronounced geometric differences between ruptured and unruptured IAs in this region. Regarding the differences in SAD and DUR between datasets 1 and 2, it is likely that differences in the patient collectives, subsample sizes, and reconstruction

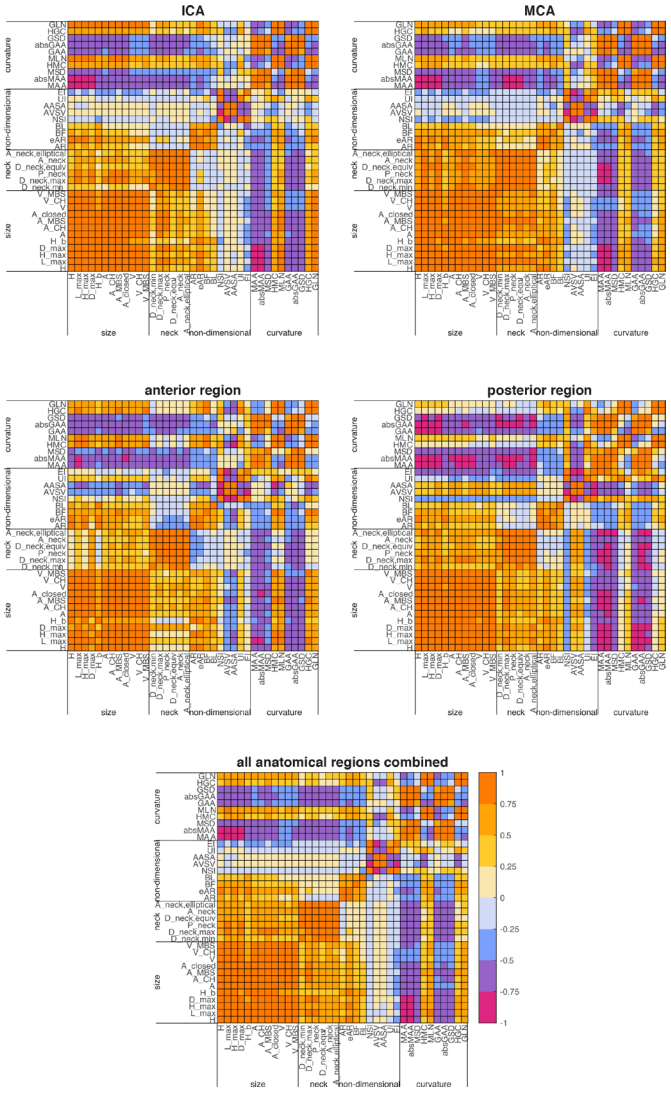

Figure 3 Pearson's r for correlation between geometric risk parameters by anatomical region for dataset 1. ICA, internal carotid artery; MCA, middle cerebral artery.

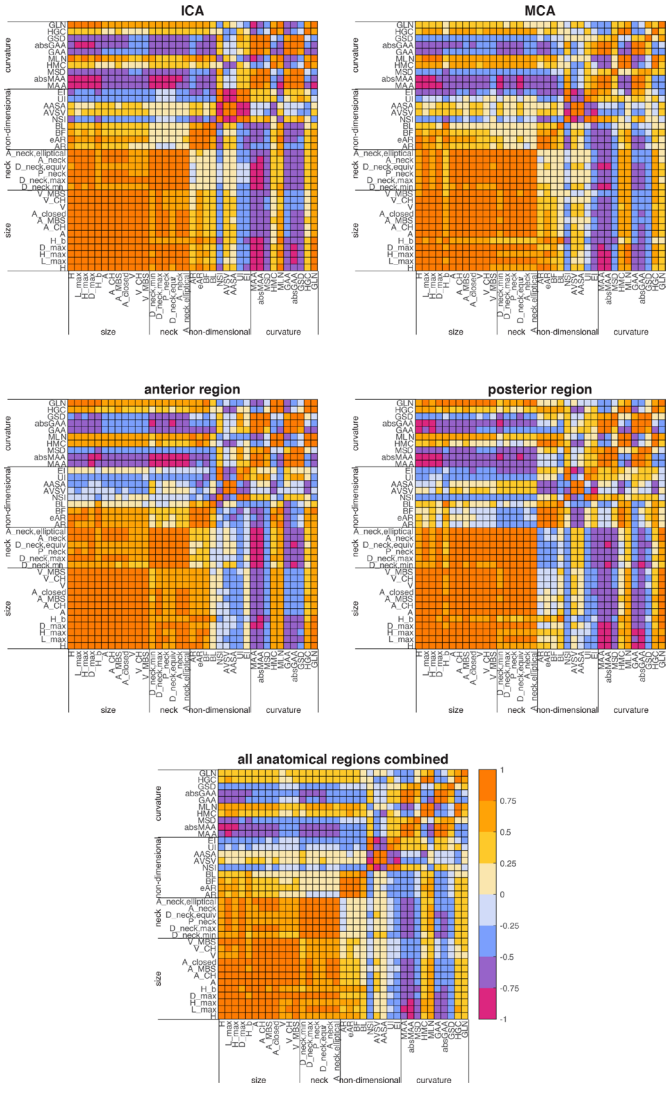

Figure 4 Pearson's r for correlation between geometric risk parameters by anatomical region for dataset 2. ICA, internal carotid artery; MCA, middle cerebral artery.

techniques are the main causes. The latter could in the future be tackled by machine learning-based segmentation methods, which can reduce operator-induced uncertainty. Examples of such methods have previously been presented, for example, in the context of the CADA challenge.[26]

Regarding the correlation patterns, there is substantial similarity between all analysed anatomical regions and datasets. Parameters tend to be most strongly correlated with other parameters from the same parameter group, except for the non-dimensional and curvature parameters, which form two subgroups each. This is reasonable, given that the parameters within each parameter group capture similar aspects of IA geometry. For the size and neck parameter groups, this is obvious, since they both capture aspects of IA and neck size, respectively. The two distinct correlation subgroups within the non-dimensional parameter group are likely caused by the underlying parameter subgroups capturing different aspects of aneurysm shape. While the parameters of the first subgroup (AR, eAR, BF, BL) are simply ratios of one-dimensional size parameters, the second subgroup (NSI, AVSV, AASA, UI, EI) is formed by parameters relating aneurysm area and/or volume to geometric reference objects, for example, the minimal bounding sphere or convex hull. The negative correlation between AVSV and AASA with the other parameters from the second subgroup is due to the parameter definitions, which cause AVSV and AASA to increase with increasing sphericity, while the other parameters tend to decrease with increasing sphericity. The curvature parameters also form two subgroups, with the first subgroup consisting of the dimensional parameters quantifying the mean or dispersion of IA surface curvature (MAA, absMAA, MSD, GAA, absGAA, GSD) and the second subgroup consisting of non-dimensional, scale invariant curvature parameters (HMC, MLN, HGC, GLN). Since the former parameters intrinsically decrease with IA size, while the latter parameters increase with IA size, the negative correlation

of the two subgroups with each other makes sense. It should be noted that the positive correlation of the non-dimensional curvature parameters with IA size is not an intrinsic property of the non-dimensional parameters themselves, since they are designed to be scale invariant. It rather indicates that curvature and irregularities of the IA surface increase in larger IAs.

For a geometric risk parameter to be a good candidate for rupture risk prediction, it should generally have a high SAD, in order to be able to differentiate between ruptured and unruptured IAs. Additionally, DUR should be high, indicating low sensitivity of the parameter to the imaging, segmentation and calculation workflow, by which it is calculated. This is desirable because it allows models including such parameters to generalise well to other datasets. Finally, when choosing a set of parameters, data from the correlation analysis can be used to identify parameters that are not strongly correlated. Neyazi *et al*[13] have previously used this method to derive a two-parameter rupture status prediction model from a set of 49 geometric and haemodynamic rupture risk parameters, identifying AR and the maximal relative residence time as the most suitable model parameters. Other attempts to identify suitable rupture status prediction models based on geometric risk parameters have been attempted, for example, Dhar *et al*[15] and Zheng *et al*,[27] but results have generally been inconsistent. Possible reasons for the discrepant findings regarding optimal parameter choice are the sample sizes used and the uncertainty inherent in the workflow by which the parameters are calculated. This may lead to the selection of less robust parameters that perform well on a given dataset but generalise less well to others. Based on the results of this study and considering SAD, DUR, as well as the correlation between geometric risk parameters, examples of more robust parameter choices could look as follows:

- H_{max}, $D_{neck,min}$, AR, AASA and MLN for the anterior region.
- L_{max}, P_{neck}, AR, AASA and HGC for the ICA.
- D_{max}, $D_{neck,min}$, eAR, AASA and HMC for the MCA.
- L_{max}, $D_{neck,min}$, BL, EI and absMAA for the posterior region.
- H_b, $D_{neck,min}$, AR, AASA, and MLN if looking at all anatomical regions combined.

Overall, while individual size, neck and curvature parameters achieved good discriminative performance and robustness, the non-dimensional parameters tended to perform well as a group. This suggests that non-dimensional geometric risk parameters can provide comparatively good discriminative performance, while the non-dimensionalisation itself mitigates some of the uncertainty introduced through the workflow by which the parameters are calculated.[14] Neither did we attempt to develop a novel aneurysm rupture risk prediction model, nor did we test earlier published models.[16 28] We decided against this analysis due to the large variety of published proposed risk models. Such models as well as the propagation of the parameters' uncertainty to the rupture risk assessment should be tested in a separate study. Finally, more elaborate models will also require further information such as hypertension status, earlier SAH as well as haemodynamic parameters, which were unavailable for this study.

Limitations

IAs were grouped by anatomical region because IA location is an important determinant of rupture risk, as demonstrated by its weight in current risk scores.[7–9] However, by analysing the datasets by anatomical region, some subsamples become quite small. Small sample size might affect the accuracy of the median and IQR estimates derived from these groups. This limitation is, however, partially mitigated by also analysing all anatomical regions combined and using two datasets, in order to get a more comprehensive picture of the risk parameters' performance. The major focus of the study was the analysis of the performance and robustness of 37 geometric risk parameters. Thus, not all findings of this study could be assessed in depth. For example, we decided to group the aneurysms by anatomical regions as recommended by clinical scores, such as such as PHASES score.[7] While we observed differences in both SAD and DUR based on the aneurysms' location within the circulation, the underlying mechanisms for these differences cannot be assessed using the available data. However, Tykocki and Kostkiewicz[29] found significant differences between some geometric parameters (parent artery size, size ratio, and aspect ratio) of aneurysms of the anterior and the posterior regions. They associated the difference in these parameters to different impacts on the intra-aneurysmal haemodynamics such as vortex formation and wall shear stress. Why these geometric parameters might result in different haemodynamic conditions and rupture risks must be investigated in a dedicated study. This is especially important as this study's findings demonstrated differences in the SAD between locations and the cohorts and when all aneurysm locations were evaluated together.

Another potential limitation is the uncertainty values from Goubergrits *et al*,[14] which were used to calculate DUR. These values were calculated on a sample containing MCA and posterior region IAs.[14] While it does not seem particularly probable, it is possible that IA location and size might affect the uncertainty inherent in calculating the geometric risk parameters in a relevant manner, which in turn could influence DUR results. Accordingly, the generalisation of MRU values from the uncertainty study[14] should be considered with caution, especially as those values were calculated only based on five aneurysms. A more fundamental limitations is the focus on geometric risk parameters. These parameters serve as proxies for the pathophysiological processes leading to IA rupture through the latter's influence on the geometry of the IA surface. Due to their nature, geometric risk parameters cannot directly capture the haemodynamic, mechanical, or biochemical aspects of IA rupture. Nevertheless, they are among the most intensely researched types of IA

rupture risk parameters, due to the comparative ease with which they can be calculated from clinical data.

All parameters included within this study have been discussed in previous literature as potential risk parameters. Note, however, that the list of parameters investigated in this study is not exhaustive. More proposed geometric parameters can be found in recent literature.[30] The parameters investigated here are limited to a set of parameters investigated earlier in frames of the uncertainty study.[14] Additionally, these parameters were constrained to parameters that can be calculated automatically.

Finally, the calculation of geometric parameters including the ostium plane depends on a sufficient reference plane selection. Recently, Berg *et al*[31] quantified the potential effect of neck curve variations on haemodynamic predictions. These findings could be transferred to the cases included in this study in future work.

Due to the retrospective nature of this work, only the parameters' capabilities to discriminate the rupture status could be assessed by comparing their respective values observed in ruptured or unruptured IA. To adequately assess the capabilities of any model using these parameters for rupture risk assessment, it has to be evaluated on a longitudinal cohort containing only UIA.

CONCLUSION

Based on datasets from two research groups, the present study provides location-specific estimates of the discriminative ability of a large set of geometric risk parameters for IA rupture status assessment, while also considering uncertainty. Additionally, correlation patterns between the parameters are identified. The presented data are potentially useful in evaluating geometric risk parameters for use in rupture risk models or when choosing input parameters for machine learning approaches to rupture risk prediction. It may also be helpful when designing future geometric risk parameters for clinical use.

Author affiliations
[1]Institute of Computer-Assisted Cardiovascular Medicine, Charité – Universitätsmedizin Berlin, Berlin, Germany
[2]Laboratory of Fluid Dynamics and Technical Flows, University of Magdeburg, Magdeburg, Germany
[3]Research Campus STIMULATE, University of Magdeburg, Magdeburg, Germany
[4]Department of Simulation and Graphics, University of Magdeburg, Magdeburg, Germany
[5]Helios Klinikum Berlin-Buch, Berlin, Germany
[6]Department of Neurosurgery, University Hospital Magdeburg, Magdeburg, Germany
[7]Department of Radiology, AMEOS Hospital Bernburg, Bernburg, Germany
[8]Department of Radiology and Neuroradiology, University Medical Center Schleswig-Holstein (UKSH), Kiel, Germany
[9]Einstein Center Digital Future, Berlin, Germany

Acknowledgements The authors kindly acknowledge PD Dr Belal Neyazi (Department of Neurosurgery, University Hospital Magdeburg) for his assistance during data acquisition as well as Adriano Schlief (Institute of Computer-assisted Cardiovascular Medicine, Charité – Universitätsmedizin Berlin) for his help in checking the topology and scaling of the intracranial aneurysm geometries.

Contributors Roles according to CRediT (contributor roles taxonomy). Conceptualisation: LG, JS, FH, JB and PB. Methodology: FH, JS and LG. Resources: AS, IES, OB, NL, SS and PB. Investigation: JB, FH and JS. Formal analysis: FH. Funding acquisition: LG, PB and SS. Supervision: LG. Writing – original draft: FH, LG and JB. Writing – review and editing: PB, SS, AS, IES, OB, NL and JS. Guarantor: FH.

Funding This study was partly funded by the Federal Ministry of Education and Research in Germany within the Forschungscampus STIMULATE (grant number 13GW0473A) and the German Research Foundation (grant number SA 3461/2-1, BE 6230/2-1).

Competing interests None declared.

Patient and public involvement Patients and/or the public were not involved in the design, or conduct, or reporting, or dissemination plans of this research.

Patient consent for publication Not applicable.

Ethics approval This study involves human participants and was approved by Ethikkommission der Charité – Universitätsmedizin Berlin: EA2/222/19 and Ethikkommission der Med. Hochschule Hannover: NOVA Nr. 68/20. In this study, only surface geometries of intracranial aneurysms that were reconstructed from clinical routine data were used. Collection of informed consent was waived by the respective institutional review boards.

Provenance and peer review Not commissioned; externally peer reviewed.

Data availability statement All data relevant to the study are included in the article or uploaded as supplementary information.

ORCID iDs
Jan Brüning http://orcid.org/0000-0002-0540-7972
Leonid Goubergrits http://orcid.org/0000-0002-1961-3179

REFERENCES

1 Vlak MH, Algra A, Brandenburg R, *et al*. Prevalence of unruptured intracranial aneurysms, with emphasis on sex, age, comorbidity, country, and time period: a systematic review and meta-analysis. *Lancet Neurol* 2011;10:626–36.
2 Brown RD, Broderick JP. Unruptured intracranial aneurysms: epidemiology, natural history, management options, and familial screening. *Lancet Neurol* 2014;13:393–404.
3 Wiebers DO, Whisnant JP, Huston J, *et al*. Unruptured intracranial aneurysms: natural history, clinical outcome, and risks of surgical and endovascular treatment. *Lancet* 2003;362:103–10.
4 Rackauskaite D, Svanborg E, Andersson E, *et al*. Prospective study: Long-term outcome at 12-15 years after aneurysmal subarachnoid hemorrhage. *Acta Neurol Scand* 2018;138:400–7.
5 Pontes FGdeB, da Silva EM, Baptista-Silva JC, *et al*. Treatments for unruptured intracranial aneurysms. *Cochrane Database Syst Rev* 2021;5:CD013312.
6 Thompson BG, Brown RD, Amin-Hanjani S, *et al*. Guidelines for the management of patients with unruptured intracranial aneurysms: a guideline for healthcare professionals from the American heart Association/American stroke association. *Stroke* 2015;46:2368–400.
7 Greving JP, Wermer MJH, Brown RD, *et al*. Development of the phases score for prediction of risk of rupture of intracranial aneurysms: a pooled analysis of six prospective cohort studies. *Lancet Neurol* 2014;13:59–66.

8 Etminan N, Brown RD, Beseoglu K, *et al*. The unruptured intracranial aneurysm treatment score: a multidisciplinary consensus. *Neurology* 2015;85:881–9.
9 Backes D, Rinkel GJE, Greving JP, *et al*. Elapss score for prediction of risk of growth of unruptured intracranial aneurysms. *Neurology* 2017;88:1600–6.
10 Juvela S. Phases score and treatment scoring with cigarette smoking in the long-term prediction of rupturing of unruptured intracranial aneurysms. *J Neurosurg* 2022;136:156–62.
11 Molenberg R, Aalbers MW, Mazuri A, *et al*. The unruptured intracranial aneurysm treatment score as a predictor of aneurysm growth or rupture. *Eur J Neurol* 2021;28:837–43.
12 Hernández-Durán S, Mielke D, Rohde V, *et al*. Is the unruptured intracranial aneurysm treatment score (UIATS) sensitive enough to detect aneurysms at risk of rupture? *Neurosurg Rev* 2021;44:987–93.
13 Neyazi B, Swiatek VM, Skalej M, *et al*. Rupture risk assessment for multiple intracranial aneurysms: why there is no need for dozens of clinical, morphological and hemodynamic parameters. *Ther Adv Neurol Disord* 2020;13:1756286420966159.
14 Goubergrits L, Hellmeier F, Bruening J, *et al*. Multiple aneurysms anatomy challenge 2018 (match): uncertainty quantification of geometric rupture risk parameters. *Biomed Eng Online* 2019;18:35.
15 Dhar S, Tremmel M, Mocco J, *et al*. Morphology parameters for intracranial aneurysm rupture risk assessment. *Neurosurgery* 2008;63:185–97.
16 Detmer FJ, Chung BJ, Mut F, *et al*. Development and internal validation of an aneurysm rupture probability model based on patient characteristics and aneurysm location, morphology, and hemodynamics. *Int J Comput Assist Radiol Surg* 2018;13:1767–79.
17 Lauric A, Baharoglu MI, Malek AM. Ruptured status discrimination performance of aspect ratio, height/width, and bottleneck factor is highly dependent on aneurysm sizing methodology. *Neurosurgery* 2012;71:38–46.
18 Berg P, Voß S, Saalfeld S, *et al*. Multiple aneurysms anatomy challenge 2018 (match): phase I: segmentation. *Cardiovasc Eng Technol* 2018;9:565–81.
19 Ma B, Harbaugh RE, Raghavan ML. Three-Dimensional geometrical characterization of cerebral aneurysms. *Ann Biomed Eng* 2004;32:264–73.
20 Ramachandran M, Retarekar R, Harbaugh RE, *et al*. Sensitivity of quantified intracranial aneurysm geometry to imaging modality. *Cardiovasc Eng Technol* 2013;4:75–86.
21 O'meara B, Rahal JP, Lauric A, *et al*. Benefit of a sharp computed tomography angiography reconstruction kernel for improved characterization of intracranial aneurysms. *Neurosurgery* 2014;10 Suppl 1:97–105.
22 Berg P, Saalfeld S, Voß S, *et al*. Does the DSA reconstruction kernel affect hemodynamic predictions in intracranial aneurysms? an analysis of geometry and blood flow variations. *J Neurointerv Surg* 2018;10:290–6.
23 Cebral JR, Castro MA, Appanaboyina S, *et al*. Efficient pipeline for image-based patient-specific analysis of cerebral aneurysm hemodynamics: technique and sensitivity. *IEEE Trans Med Imaging* 2005;24:457–67.
24 Sarrami-Foroushani A, Lassila T, Frangi AF. Virtual endovascular treatment of intracranial aneurysms: models and uncertainty. *Wiley Interdiscip Rev Syst Biol Med* 2017;9:wsbm.1385.
25 Schneiders JJ, Marquering HA, Antiga L, *et al*. Intracranial aneurysm neck size overestimation with 3D rotational angiography: the impact on intra-aneurysmal hemodynamics simulated with computational fluid dynamics. *AJNR Am J Neuroradiol* 2013;34:121–8.
26 Ivantsits M, Goubergrits L, Kuhnigk J-M, *et al*. Detection and analysis of cerebral aneurysms based on X-ray rotational angiography - the CADA 2020 challenge. *Med Image Anal* 2022;77:102333.
27 Zheng Y, Xu F, Ren J, *et al*. Assessment of intracranial aneurysm rupture based on morphology parameters and anatomical locations. *J Neurointerv Surg* 2016;8:1240–6.
28 Lall RR, Eddleman CS, Bendok BR, *et al*. Unruptured intracranial aneurysms and the assessment of rupture risk based on anatomical and morphological factors: sifting through the sands of data. *Neurosurg Focus* 2009;26:E2.
29 Tykocki T, Kostkiewicz B. Aneurysms of the anterior and posterior cerebral circulation: comparison of the morphometric features. *Acta Neurochir* 2014;156:1647–54.
30 Juchler N, Schilling S, Bijlenga P, *et al*. Shape Trumps size: image-based morphological analysis reveals that the 3D shape discriminates intracranial aneurysm disease status better than aneurysm size. *Front Neurol* 2022;13:809391.
31 Berg P, Behrendt B, Voß S, *et al*. Victoria: virtual neck curve and true ostium reconstruction of intracranial aneurysms. *Cardiovasc Eng Technol* 2021;12:454–65.
32 Lauric A, Miller EL, Baharoglu MI, *et al*. 3D shape analysis of intracranial aneurysms using the Writhe number as a discriminant for rupture. *Ann Biomed Eng* 2011;39:1457–69.
33 Chien A, Sayre J, Viñuela F. Comparative morphological analysis of the geometry of ruptured and unruptured aneurysms. *Neurosurgery* 2011;69:349–56.
34 Ujiie H, Tamano Y, Sasaki K, *et al*. Is the aspect ratio a reliable index for predicting the rupture of a saccular aneurysm? *Neurosurgery* 2001;48:495–503.